Fuel effect on solution combustion synthesis of Co(Cr,Al)$_2$O$_4$ pigments

Jessica Gilabert [a,*], Maria Dolores Palacios [b], Vicente Sanz [b,c], Sergio Mestre [b,c]

[a] Instituto de Tecnología Cerámica, Asociación de Investigación de las Industrias Cerámicas, Castellón, Spain
[b] Instituto Universitario de Tecnología Cerámica, Universitat Jaume I, Castellón, Spain
[c] Departamento de Ingeniería Química, Universitat Jaume I, Castellón, Spain

ARTICLE INFO

ABSTRACT

The fuel effect on the synthesis of a ceramic pigment with a composition CoCr$_{2-2\Psi}$Al$_{2\Psi}$O$_4$ ($0 \leq \Psi \leq 1$) by means of solution combustion synthesis process (SCS) has been studied. Three different fuels were selected to carry out the synthesis (urea, glycine and hexamethylen-tetramine (HMT)). Highly foamy pigments with very low density were obtained. Fd-3m spinel-type structure was obtained in all the experiments. Nevertheless, crystallinity and crystallite size of the spinels show significant differences with composition and fuel. The use of glycine along with the chromium-richest composition favours ion rearrangement to obtain the most ordered structure. Lattice parameter does not seem to be affected by fuel, although it evolves with Ψ according to Vegard's law.

Colouring power in a transparent glaze shows important variations with composition. On the other hand, fuel effect presents a rather low influence since practically the same shades are obtained. However, it exerts certain effect on luminosity (L^*).

Efecto del combustible en la síntesis de pigmentos Co(Cr,Al)$_2$O$_4$ por combustión de una disolución

RESUMEN

Se ha estudiado el efecto del combustible en la síntesis de pigmentos cerámicos tipo CoCr$_{2-2\Psi}$Al$_{2\Psi}$O$_4$ ($0 \leq \Psi \leq 1$), obtenidos mediante síntesis por combustión de una disolución. Se seleccionaron 3 tipos de combustible diferentes: urea, glicina y hexametilentetramina. Todos los pigmentos obtenidos presentaron una textura altamente esponjosa y con muy baja densidad. Las estructuras cristalinas desarrolladas en todos los casos fueron tipo espinela Fd-3m. Sin embargo, tanto la cristalinidad como el tamaño de cristalito presentaron dife-rencias significativas dependiendo de la composición y del combustible utilizado. El uso de glicina, junto con las composiciones más ricas en cromo, favorece la reorganización de los iones para obtener estructuras más ordenadas y con mayor cristalinidad. El parámetro de red no parece verse afectado por el combustible, aunque sí evoluciona con Ψ de acuerdo con la Ley de Vegard.

El poder colorante desarrollado por los pigmentos, una vez introducidos en un esmalte cerámico transparente, muestra variaciones importantes por el efecto de la composición. Por el contrario, prácticamente no se aprecia el efecto del combustible, ya que se obtienen tonos de color similares entre las muestras. Sin embargo, sí es posible destacar cierto efecto sobre el componente responsable de la luminosidad.

Introduction

Traditionally, ceramic pigments have been obtained by means of a long-established process which involves solid state reactions between oxides. The technology requires applying really high temperatures ($\sim$1300 °C) and long soaking times [1] which results in pigments with high particle sizes which need an intensive grinding. As a consequence, new wet-chemical methodologies have been recently developed in order to overcome these limitations of the traditional ceramic process. Some authors have studied in depth the sol-gel route [2,3], the co-precipitation method [4,5] as well as other alternative routes like the polymeric precursor method [6–8]. These advanced processes allow controlling the stoichiometry as well as obtaining well-developed spinel-type structures with high purity, which fosters an improvement in the colouring power.

Solution combustion synthesis (SCS) has emerged as an innovative wet-chemical method to synthesize ceramic materials like pigments. Low-particle size products are obtained by means of SCS, using short reaction times and moderate temperatures [9]. This synthesis technique is suitable to overcome some important disadvantages of the traditional process. From an economic and technical point of view, SCS involves lower preparation costs, as is easy to scale up. In addition, SCS generates very homogeneous pigments as foamy masses made up of nanosized grains, without needing a further intense milling process. This last property makes SCS pigments really useful for inkjet technology which requires submicronic particle sizes.

SCS synthesis is carried out by mixing a concentrated aqueous solution of precursors (nitrates are frequently used) with a specific fuel (urea, hexamethylentetramine, glycine, hydrazine and their derivates, etc.). After stirring the solution to mix the reactants at atomic scale, water is evaporated in a fast-heating process up to 500 °C so that the remaining solid sediment ignites to burn spontaneously in a highly exothermic reaction, providing enough energy to synthesize the desired product. The release of large quantities of gases during the reaction (CO_2, H_2O and N_2) generates a product with a foamy appearance.

SCS is a broadly used technique to synthesize large number of inorganic materials, either simple or mixed oxides [10–15]. Spinels are one of the most characteristic group SCS has worked in [9], because a relevant number of pigments included in CPMA classification, have this structure [16]. Spinel-type materials have been perfectly developed using SCS method according to what Patil et al. [17,18], Costa et al. [19], Ianoş et al. [20] or Mimani and Ghosh [21] have reported. In addition, Mestre et al., in previous works, demonstrated that SCS was also adequate to synthesize complex spinels using urea as fuel [22,23].
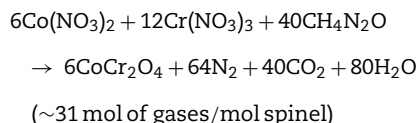
Many variables must be considered when developing a new pigment by SCS: mixture composition, fuel, solution concentration or even thermal treatment is some of the most important [24,25]. The selection of the suitable fuel is supposed to be a critical parameter because it is responsible for modifying the mechanism and kinetics of the combustion and, consequently, it grants the possibility to control the product characteristics. Many fuels are reported to ignite a SCS mixture, being the urea the most frequently used by their low cost and harmlessness. However, every fuel could act in different ways and, as a consequence, its influence in the final product's properties should be analyzed. There are no systematic studies about the feasibility of selecting the right fuel to develop new or improved spinel pigments with higher colouring power. As a consequence, this research is aimed to study the synthesis of mixed spinels $Co(Cr,Al)_2O_4$ to evaluate the fuel influence into the pigment final properties (mainly crystallinity and tinting strength). Green $CoCr_2O_4$ and blue $CoAl_2O_4$ were the original spinels selected to develop the study because they are two of the most characteristic spinels used in the traditional ceramic industry [26,27].
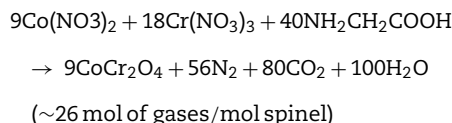
Materials and methods

Samples were formulated following the general formula $CoCr_{2-2\psi}Al_{2\psi}O_4$ ($0 \leq \Psi \leq 1$ in steps of 0.2). Three different fuels were selected in order to study the effect of the fuel nature in the synthesis of the pigments, urea (CH_4N_2O), glycine (NH_2CH_2COOH) and hexamethylentetramine (HMT, $C_6H_{12}N_4$). They are the most popular and attractive fuels to yield highly uniform, complex oxide ceramic powder with precisely controlled stoichiometry.

The molar reaction for one of the composition with each fuel is shown as an example:

Spinel reaction using urea as a fuel:

$$6Co(NO_3)_2 + 12Cr(NO_3)_3 + 40CH_4N_2O$$

$$\rightarrow 6CoCr_2O_4 + 64N_2 + 40CO_2 + 80H_2O$$

($\sim$31 mol of gases/mol spinel)

Spinel reaction using glycine as a fuel:

$$9Co(NO3)_2 + 18Cr(NO_3)_3 + 40NH_2CH_2COOH$$

$$\rightarrow 9CoCr_2O_4 + 56N_2 + 80CO_2 + 100H_2O$$

($\sim$26 mol of gases/mol spinel)

Spinel reaction using HMT as a fuel:

$$36Co(NO_3)_2 + 72Cr(NO_3)_3 + 40C_6H_{12}N_4$$

$$\rightarrow 36CoCr_2O_4 + 224N_2 + 240CO_2 + 240H_2O$$

($\sim$20 mol of gases/mol spinel)
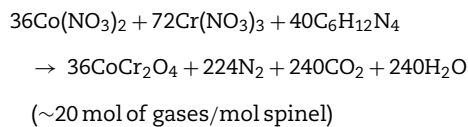
The precursor nitrates from the corresponding metal ions of each composition and the selected fuel were weighted following the reaction stoichiometry and dissolved in 50 mL of distilled water (all reactants from Panreac Química, S.A.U., Spain). Three different series of data were obtained depending on the fuel used. In the first series of experiments 24 g of urea were used. The second series was carried out with 20 g of glycine and the third one with 9.3 g of HMT.

The aqueous solution contained in a 700 mL Pyrex dish was inserted into a muffle furnace stabilized at 500 °C (BLF 1800, Carbolite Furnaces Ltd, UK). The sample was maintained 20 min at maximum temperature before cooling the kiln camera to ambient temperature (Fig. 1). During soaking time, the sample dries, boils, foam ignites and burns achieving temperatures around 1500 °C [9]. When the furnace is opened, the product presents a spongy aspect, and practically all the container volume is fulfilled. Finally, the pigment was milled for 15 min in a ball mill, using agate jars and water as a fluid (Pulverisette 5, Fritsch GmbH, Germany).

The mineralogical characterization of the structures was carried out by XRD (Theta-Theta D8 Advance, Bruker, Germany), with CuKα radiation (λ = 1.54183 Å). The generator settings were 45 kV and 40 mA. The XRD data were collected in a 2θ of 5–90° with a step width of 0.015° and a counting time of 1.2 s/step by means of a VÅNTEC-1 detector. The diffraction patterns were treated by the Rietveld analysis program DIFFRACplus TOPAS (4.2 version), assuming a pseudo-Voight function to describe peak shapes. The refinement protocol included the background, the scale factors and the global-instrument, lattice, profile and texture parameters. In addition, simultaneous thermal analyses were carried out to assure the perfect development of combustion. Both differential and thermogravimetric analyses were conducted using a TGA-SDTA 851E/160 (Mettler Toledo, Switzerland). Approximately 20 mg of the samples were weighted in a platinum vessel and subjected to a thermal treatment from 25 to 1000 °C at 10 °C/min of heating rate using a dynamic air atmosphere (50 mL/min flow).

The evolution of sample morphology was studied carrying out microstructural and particle size tests. Sample microstructure was analyzed by means of FEG-SEM technique (QUANTA 200F, FEI Co, USA). Energy-dispersive X-ray microanalysis instrument (Genesis 7000 SUTW, EDAX, USA) coupled to the FEG-SEM was used to determine pigment's chemical composition. Particle size distribution was determined using laser diffraction equipment (Mastersizer 2000, Malvern Instruments Ltd, UK). The size distribution was calculated using the MIE theory in order to interpret the light scattering signal collected by the detectors. The calculations were made considering the refractive index of the pigment (RI) and their absorption coefficient value (CoCr$_2$O$_4$ RI = 2.08, C$_{abs}$ = 1; CoAl$_2$O$_4$ RI = 1.74,

C$_{abs}$ = 0.1). A wet dispersion of the samples was used. The sample was mixed in a hexametaphosphate diluted solution to disperse the particles. A 5-min ultrasonic bath was further applied in order to completely individualize the particles. Finally, the sample was mechanically stirred before it was fed into the instrument.

The colouring power of every sample was measured by inserting the pigments in 2/98 wt.% proportion into a transparent glaze (classified as a single-fired porous tile glaze with 0.5% Na$_2$O, 4.0% K$_2$O, 15.3% CaO, 0.9% MgO, 9.0% ZnO, 7.4% Al$_2$O$_3$, 3.0% B$_2$O$_3$, 59.5% SiO$_2$ chemical composition). Immediately, a fired wall tile was coated with this mixture, which were fired together in an electric laboratory kiln according to a thermal cycle of single-fired floor tiles (maximum temperature 1100 °C and 6 min of soaking time). The spectrophotometric curve and CIELab chromatic coordinates of the glazes were determined using CIE Illuminant D$_{65}$ and CIE 10° standard observer (Color Eye 7000A, X-Rite Inc., USA).

Results and discussion

The synthesis experiments generated products with a foamy aspect, which occupied the whole volume of the combustion container. These products presented homogeneous and intense colours, not being observed any gradient in the whole spongy volume which pointed to some kind of ion segregation. Colour palette ranged from light greens, passing through dark green until obtaining intense blues. Pigments showed no difficulties to disaggregate until obtaining a finely grained powder.

Crystalline structure

XRD results show that all as-formed pigments had developed spinel structure (Fd-3m, face centred cubic crystal structure), characteristic of the target ceramic pigments [28], independently of composition and fuel (Fig. 2). In practically all samples, there is no evidence of additional peaks related to non-reacted oxides or other intermediate reaction products which could be formed instead of the spinel structure. Only in the sample with Ψ = 1 carried out with glycine the presence of an aluminium hydroxide in low proportions was identified, but it did not appear again in the rest of samples. This phase could be present because of some aluminium cation that had not been completely integrated in the spinel structure during combustion, remaining as a very reactive alumina, which was hydrated during the wet milling. Nevertheless, its weight proportion was barely noticeable, practically less than 5 wt.% and there was no a repetitive pattern observed in the rest of compositions. Thus, it is possible to consider that the combustion process among components was carried out in a highly effective way.

Despite developing the same spinel-type structure, a noticeable effect on crystallinity depending on the composition and fuel has been clearly produced. The developed structures show higher crystallinity when their composition was near to CoCr$_2$O$_4$ (Ψ = 0) and it progressively decreases as the amount of Al^{3+} ions enriches the composition, independently of the fuel selected. As matter of fact, crystallinity
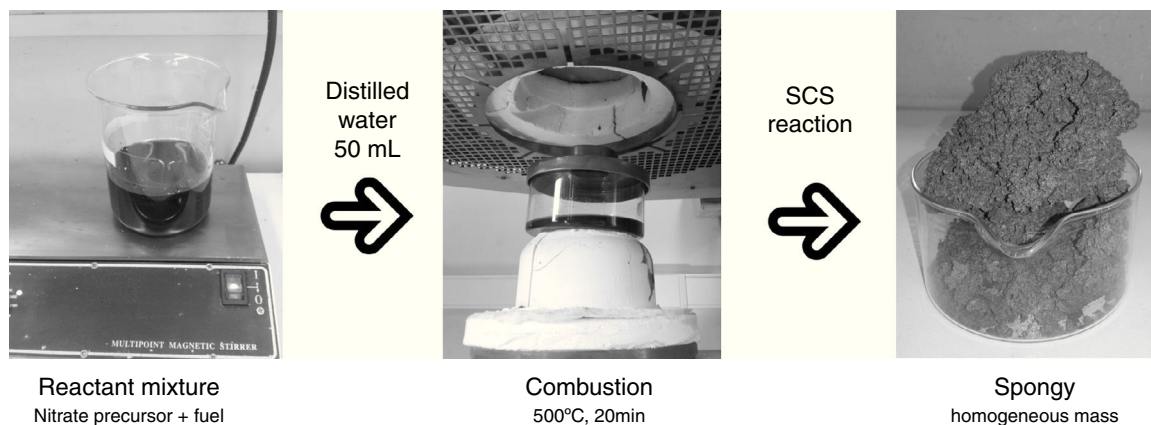
Fig. 1 – Scheme to detail experimental method to synthesize pigments by SCS.

is considerably reduced as Ψ grows until obtaining a low-crystallinity product when the composition reaches $\Psi = 1$. It means that pure spinel $CoAl_2O_4$ presents the lowest capacity of crystallization for the same combustion conditions. Furthermore, it is observed a progressive evolution of the characteristic angle towards higher values, being more pronounced as the crystallinity of the sample decreases. As reported in previous works [22], the low crystallinity for $CoAl_2O_4$ spinel is caused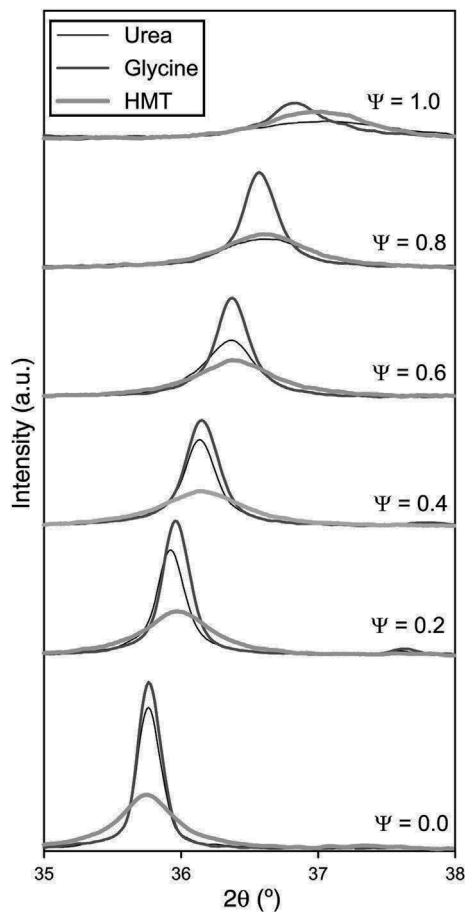 by the fast kinetics of the reaction that prevents the cation reorganization, and consequently it makes it difficult to crystallize. This phenomenon happens in a more pronounced way as spinels are richer in aluminium.

Fuel has an important effect over crystallinity. Either the areas or the peak heights in Fig. 2 are evidently dependent of the fuel used in the synthesis process. Glycine favours the spinel-structure formation since allows to obtain pigments with the highest crystallinity for every composition. Even when pure $CoAl_2O_4$ spinel is synthesized, glycine leads to certain crystallinity that was impossible to obtain with the other fuels. By the contrary, HMT is the fuel less prone to spinel crystallization as the pigments obtained with HMT show the lowest peak intensity for compositions that crystallizes with the other two fuels. However, the decreasing crystallinity of the obtained pigments with Ψ is practically regular in all compositional range, not being observed too pronounced changes in any case. Finally, the behaviour of urea is intermediate between the other fuels. Urea's effect is similar to glycine's for the compositions richer in Cr ($\Psi \leq 0.4$), but for compositions richer in Al its effect resembles to HMT.

A decrease in crystallite size of the pigments was observed as their aluminium content grows (Fig. 3). The evolution was more important when glycine and urea were used, while the HMT fuel showed a smooth reduction, practically constant, without any noticeable variation of crystallite size. The most remarkable trend is the glycine curve. A substantial decrease of crystallite size is observed as Ψ increases, until reaching an inflexion point when the pigment runs out of chromium in the structure ($\Psi = 1$). Thus, the combination Cr-glycine is the optimum to obtain the highest crystallite sizes (the most favourable case develops sizes around 100 nm) and favour spinel crystallization. No spinel-type structure obtained by means of SCS combustion, reported until this moment, had reached so considerable crystallite sizes [9].

The mechanism of pigment formation is different depending on the selected fuel. Concretely, the three of them act as fuels being decomposed with frothing as a result of the formation of $Co/(Al, Cr)(OH)(NO_3)_2$ gel along with other secondary products like urea nitrate, biuret, HNCO and NH_3 [9,24,25]. The mixture then foams due to the formation of gaseous decomposition products as intermediates, yielding to enormous swelling. These gas products are hypergolic in contact
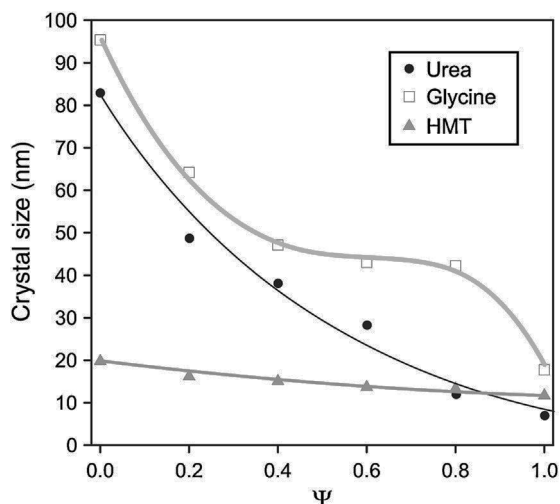

Fig. 2 – Evolution of the XRD's main reflection (I_{100}) of the pigments versus Ψ and fuel.

Fig. 3 – **Evolution of crystallite size depending on parameter Ψ.**

Fig. 4 – **Comparison of cell parameters of the spinel with the prediction of Vegard's law, based on the ICCD data from the spinels CoCr$_2$O4 ($\Psi = 0$) and CoAl$_2$O$_4$ ($\Psi = 1$).**

with each other and, as a result, the foam they develop breaks out with a flame because of their generation (flame temperature ranging from 1100 to 1500 °C). The whole foam further swells and heats to incandescence, generating the pigment spinel structure. The main difference between fuels lies in the molar ratio of emitted gases/spinel formed. The higher the amount of gaseous products released during combustion, the higher the porous voluminous masses are obtained, but the lower the maximum temperature they achieve in the process because they loss more heat. In the case of urea, glycine and HMT, the ratio is approximately 31, 26 and 20 mol gas/spinel respectively. In addition, the case of glycine is even more complex because it adds another effect in the combustion process since it complexes the metal cations (Co, Cr, Al) increasing their solubility and preventing selective precipitation as the water evaporates [29]. Crystallinity evolution observed in Figs. 2 and 3 can be explained according to these dissimilarities among fuels since their evolution during the combustion reaction alters the properties of the resulting products. In this case, the glycine process yields spinels with high crystallinity because it favours the atomic contact among metal ions to develop spinel structure.

On the other hand, certain correlation between the fluffy aspect and crystallinity grade was observed, but further studies have to be carried out in order to explain this phenomenon. No clear conclusion was obtained with only the CoCr$_{2-2\psi}$Al$_{2\psi}$O$_4$ system.

Spinel's lattice parameters show no remarkable differences when fuel was modified and are a linear function of composition (Fig. 4), which was in accordance to the theoretical behaviour defined for solid solutions by Vegard's law. Concretely, lattice parameters calculated range from theoretical values of pure spinel CoCr$_2$O$_4$ (reported value 8.33 Å [30]) to the CoAl$_2$O$_4$ values (8.06 Å [31]), whose behaviour is consistent with the higher ionic radius of the Cr^{3+} ion (0.62 Å) with respect to the Al^{3+} ion (0.39 Å [32]).

The coincident lineal trend observed for all fuels points out that spinel unit cell does not depend on the nature of
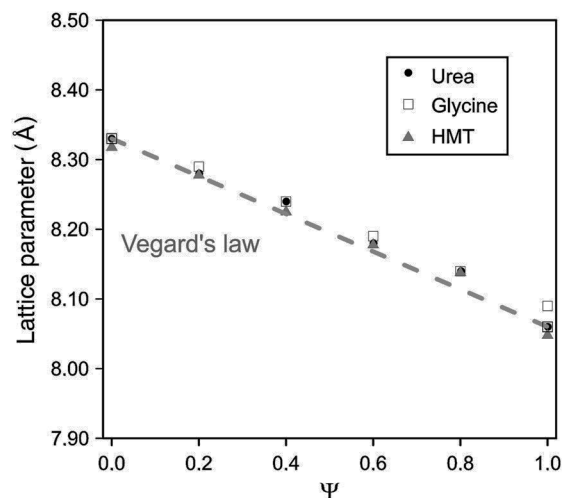
the fuel added to the system but on the nitrates mixture composition and, more concretely, on the ionic radius of the elements. In previous works carried out by Mestre et al. [23] and other authors [33,34] no lineal trends were observed in mixed spinels. On the contrary, all cases deviate somehow sharply from the Vegard's law.

Thermal analysis

XRD analysis identified additional crystalline phases apart from spinel in one case ($\Psi = 1$ and glycine). So that, in order to verify the thermal stability of the pigments developed during the SCS synthesis, a simultaneous thermal analysis was carried out on the pigments obtained with the most extreme compositions ($\Psi = 0$ and $\Psi = 1$) for all fuels. The CoCr$_2$O$_4$ pigments, which have higher crystallinity and crystallite size, hardly experience a loss of mass and no significant endothermic or exothermic transitions are observed during the test (Fig. 5a). Nevertheless, the thermal behaviour of CoAl$_2$O$_4$ was completely different because important mass changes were observed (around 15 wt.%), associated to endothermic peaks (Fig. 5b). This difference pointed out that not all synthesized pigment rearranges completely in spinel-type structure, but other phases can appear. Moreover, taking into account DTA curves for the $\Psi = 1$ pigments, two characteristic endothermic peaks are observed, independently of the fuel used. The first endothermic peak appears around 100 °C, which could be related to adsorbed water. The second peak, and more important as far as the reaction development is concerned, is registered at approximately 270 °C. This peak is attributed to the presence of aluminium hydroxide in the pigments since it is associated with the loss of OH$^-$ groups [35]. This aluminium hydroxide phase was identified by XRD in one of the samples, but the STA test corroborated the suspicious that this compound is also present in the pigments with the same nominal composition, but in a nearly amorphous state, or in a proportion under the detection limit of XRD.
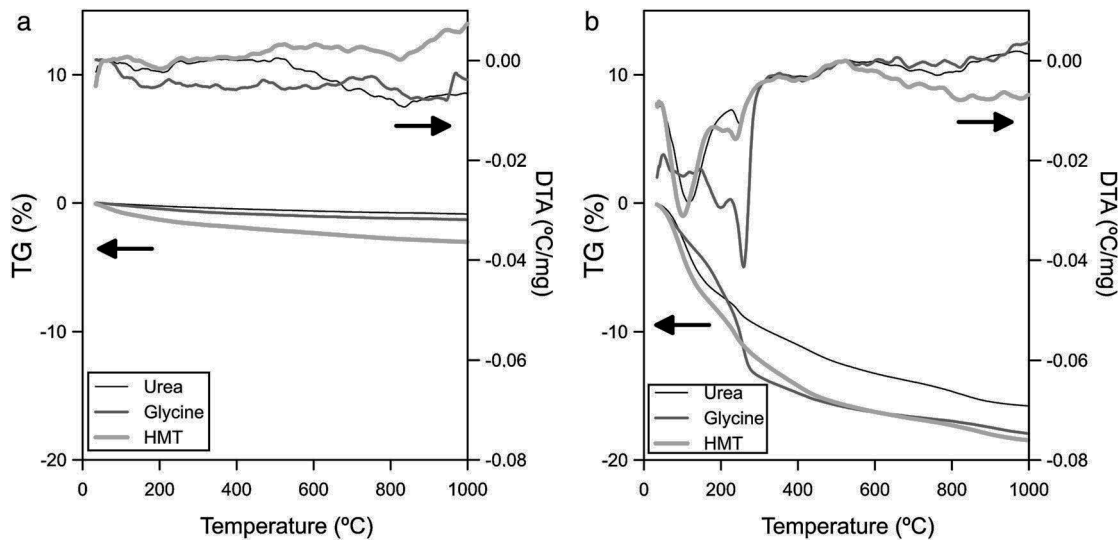
Fig. 5 – Simultaneous thermal analysis of the two pure spinels and with the three fuels: (a) CoCr$_2$O$_4$ ($\Psi = 0$), (b) CoAl$_2$O$_4$ ($\Psi = 1$).

According to STA results, none of the fuels allows to obtain exclusively spinel structure for compositions with $\Psi = 1$, because it has been clearly demonstrated that some aluminium oxide remains in combustion's product and, consequently, it became hydrated during the wet-milling process. Thus, hydroxides are generated and the pigment thermal stability reduces considerably. Nevertheless, it must be said that the presence of hydroxides is not a severe inconvenient in colour development since these crystal phases are decomposed at low temperatures, avoiding the generation of any kind of defect on the final glaze surface. However, it is a factor to take into account for the process scale-up because it has been confirmed that the lower the crystallization is, the lower the likelihood to obtain a monophasic product with all ions integrated.

Morphological characterization

A morphological analysis of the extreme spinels ($\Psi = 0$ and $\Psi = 1$) was carried out in order to identify the shape and size of the nanostructures developed during the synthesis. The MEB micrographs showed that composition and fuel influence the microstructure of the pigments (Fig. 6). The structure of CoCr$_2$O$_4$ pigment synthesized with urea ($\Psi = 0$), consisted of well-sintered submicronic round-shaped grains. The rounded morphology of grains was maintained in the samples obtained with the two other fuels, but the densification decreased in the order urea > HMT > glycine. As a consequence, glycine generated a product with a more open structure. In addition, HMT generates the grains with lower size, and it seems that they were small cracks between them. The CoAl$_2$O$_4$ pigment ($\Psi = 1$) showed a broader range of microstructures. The samples obtained with urea and HMT presented laminar-shape grains with an appreciable porosity between them, being of higher size the grains and the pores obtained with HMT. By contrast, glycine generated a pigment with mainly rounded but also prismatic grains, with lower porosity.

Table 1 – Physical characterisation of extreme pigments ($\Psi = 0$ and $\Psi = 1$) with the three fuels: specific surface area and characteristic diameters from particle size distribution.

Composition	Fuel	S_e (m^2/g)	d_{10} (µm)	d_{50} (µm)	d_{90} (µm)
$\Psi = 0$	Urea	11.8	1.1	8.8	20.8
	Glycine	10.4	0.8	5.5	16.4
	HMT	44.6	1.3	8.8	20.4
$\Psi = 1$	Urea	221	1.6	6.0	18.9
	Glycine	95	2.4	8.5	21.4
	HMT	196	2.1	9.4	26.4

All observations correlated with crystallinity behaviour and, at the same time, with specific surface area results are shown in Table 1. Specific surface area was considered as an important parameter which allows the detection of microstructural changes in pigments. In the light of the results, the higher the sample crystallinity, the bigger the grain size and more rounded his shape, being directly correlated with low specific surface area values. This phenomenon was justified because the described grains were forming agglomerates with low porosity and smooth surfaces. On the contrary, when morphology consisted of laminar-shaped grains ($\Psi = 1$) and a reduced thickness, the samples were sintered in a different way and resulted in porous agglomerates, favouring a sharp increase in specific surface area. As a result, it can be concluded that Cr-rich spinels synthesized with glycine promote the highest crystallization of the pigment, allowing spinels to develop a spongier aspect with the lowest specific surface area. On the other hand, low-crystallinity spinels (Al-rich pigment with urea of HMT) generate high specific surface area pigments because of the laminar shape of the grains, and the high porosity.

The particle size distribution of the wet-milled samples ($\Psi = 0$ and $\Psi = 1$) was also measured. Characteristic diameters from cumulative sample size distribution are shown in Table 1. Diameters d_{10}, d_{50} and d_{90} are the cut-off size particle below
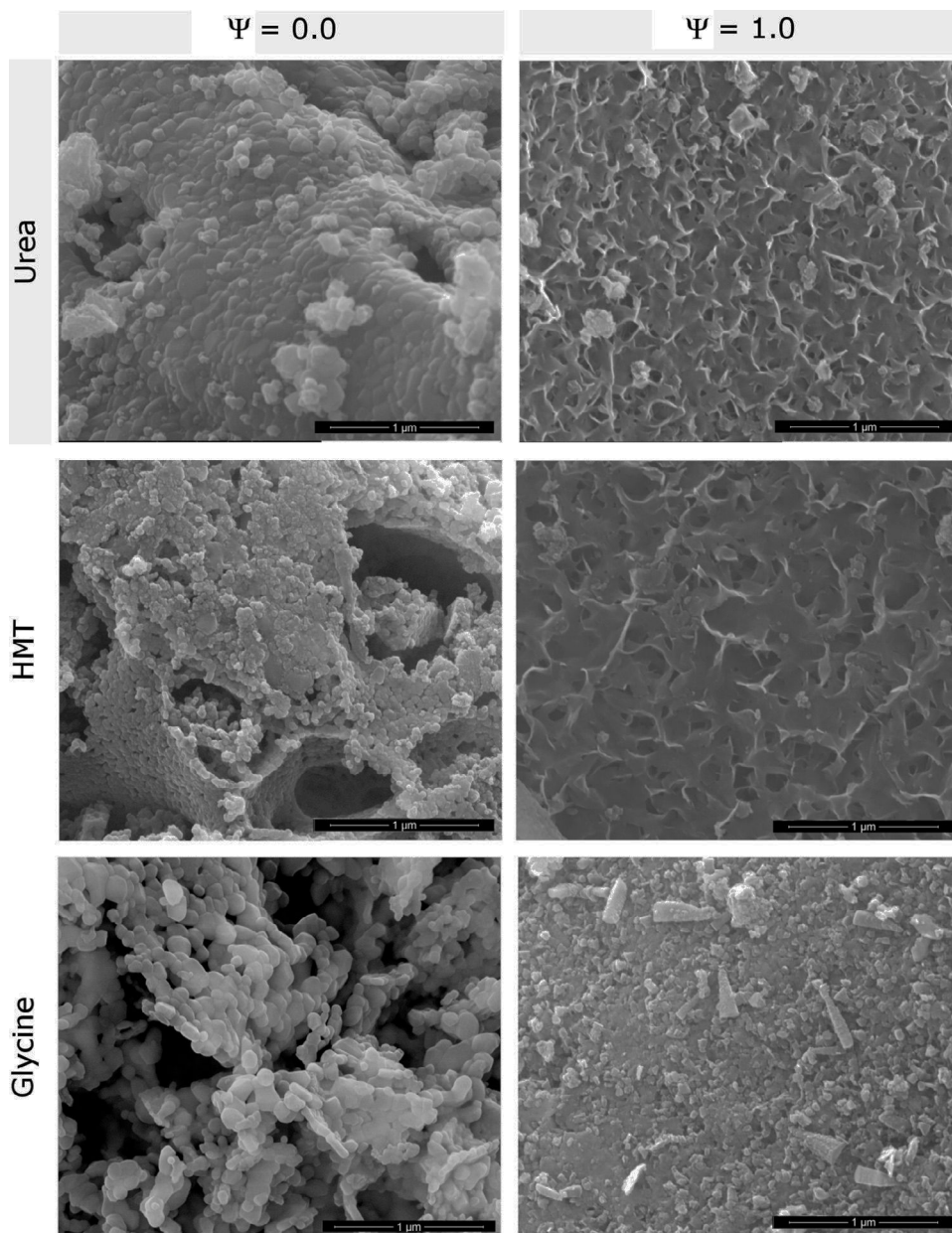
Fig. 6 – SEM micrographies obtained for simple pigments ($\Psi = 0$ and $\Psi = 1$) depending on the used fuel.

which 10%, 50% and 90% of the total particles volume lies. As reported, particle size is an important parameter to control in pigments. To give a good tinting strength, ceramic pigments should have an optimum particle size of 1–10 μm and possess a high refractive index (1.8–2.0) [9]. Both conditions are accomplished by synthesized pigments in this report, since the average particle diameter was around 8 μm in all cases and no significant differences were observed. It means that final particle size is basically controlled by the milling process and not by the synthesis parameters. Probably, if the particle size interval corresponding to inkjet inks would have been reached, the differences in the microstructure of the pigments will have been reflected in the particle size distribution of the pigments.

Parameters of particle size and specific surface area evolve in a different way. The reason lies in the porosity of particles. The most crystalline samples showed a practically smooth surface of particles (agglomerates of grains), but the less crystalline samples presented a significant intergrain porosity responsible for increasing specific surface area [36], as it can be seen in Fig. 6.

As mentioned before, both the dissimilar morphological microstructure and the differences observed in the grain size are the result of the way the fuels act during combustion. The main factors are the quantity of emitted gases and the homogeneity of ions in the mixture. In addition, higher flame temperature is reported to be responsible for particle's sintering [25]. Considering that a spongy microstructure is highly

Table 2 – Atomic composition of $CoCr_2O_4$ spinels measured in the outside and inside parts of the particles.

Composition	Fuel	Co (at.%)	Cr (at.%)	O (at.%)	Particle zone
$\Psi = 0$	Urea	26	11	63	Outside
		28	14	59	Inside
	Glycine	24	12	64	Outside
	HMT	23	13	64	Outside
		28	14	58	Inside
Theoretical value for $CoCr_2O_4$ spinel		28	14	57	

Table 3 – Atomic composition of $CoAl_2O_4$ spinels.

Composition	Fuel	Co (at.%)	Al (at.%)	O (at.%)
$\Psi = 1$	Urea	26	13	61
	Glycine	24	11	65
	HMT	25	13	62
Theoretical value for $CoAl_2O_4$ spinel		29	14	57

recommendable for ceramic pigments intended to inkjet inks because they could be milled with a lower effort, glycine seems to be the choice for developing spinel pigments with SCS method, since it allows obtaining pigments spongier than with the other investigated fuels.

Chemical analysis

EDX analyses were carried out in the most extreme compositions ($\Psi = 0$ and $\Psi = 1$), in order to check the effectiveness of the SCS method from the chemical point of view. Previous reports conducted in this regard have already demonstrated a fairly good correlation between theoretical and experimental composition of the solid solutions between spinels synthesized by SCS [23]. Tables 2 and 3 show the molar percentage of both extreme spinels versus the fuel used. According to results, both compositions presented oxygen contents higher than theoretical values. In addition, during the study of $CoCr_2O_4$ spinels, it was observed the presence of zones inside the particles which had a different composition from the one measured at the surface (Fig. 7). In these internal zones, the composition increased their cobalt and chromium content, practically equalling the theoretical values. This effect was not evidenced in Al-rich composition

An interpretation can be proposed for the facts described. The wet-milling process causes hydration of the particles, and consequently an increase in oxygen content. However, this phenomenon only affects the surface of $CoCr_2O_4$ particles as their interior has nearly the expected composition. On the contrary, the hydration is more significant in $CoAl_2O_4$ particles, due to the presence of a fraction of unreacted alumina. This hypothesis is consistent with the STA results, which showed a clear loss of mass in $CoAl_2O_4$ samples, but very small loss in $CoCr_2O_4$ samples. In addition, no significant differences were observed among samples when fuel effect was compared. This also suggests that differences in chemical analysis are due to a later stage to the synthesis.

Results indicate that SCS is an effective method for synthesizing spinels with high chemical homogeneity. However, wet-milling may cause the hydration of the less crystallized
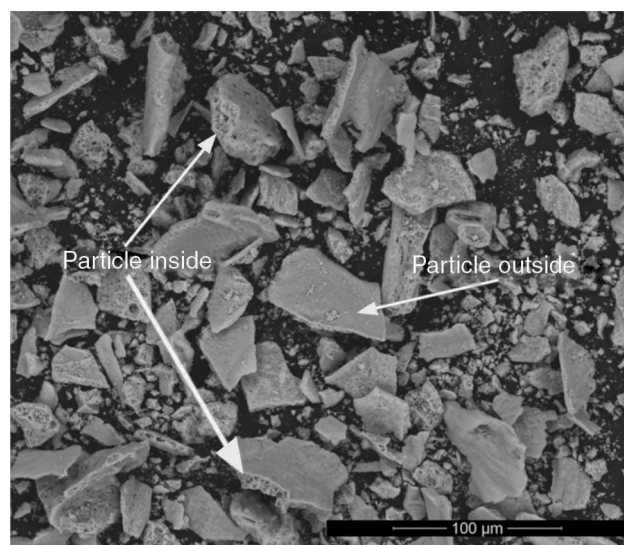

Fig. 7 – Micrography obtained for $\Psi = 0$ with urea as fuel showing the two different parts of the particles: inside and outside.

fraction, increasing the proportion of oxygen respect to the theoretical.

Determination of colouring power

Highly intense colours were obtained when adding synthesized pigments into the ceramic glaze. Neither colour loss nor attenuation was observed in any of the samples. Thus, developed spinels showed high stability against the glaze during firing (which can be highly aggressive with pigment structures). In addition, no visual defects (like pinholes) or colour heterogeneities were present in the glazed samples. As a consequence, all synthesized spinels worked suitably as ceramic pigments, independently of the fuel used (which is related with crystallinity, crystal size or specific surface).

Obtained tones covered a wide colour palette from light green ($\Psi = 0$), passing through darker greens, to intense blue ($\Psi = 1$). The pigments obtained with the three fuels presented

a similar colour evolution with Ψ, a trend which was confirmed by the reflectance curves (Fig. 8). In consequence, the differences in crystallinity, crystal size or specific surface, exert little influence on the colouring power.

Broadly speaking, the evolution of the spectrophotometric curves can be interpreted considering that the Al^{3+} ion substitutes the Cr^{3+} ion. As a consequence, the broad but subtle absorption band between 350 and 550 nm, which is typical of green Cr-spinels, evolves to a better defined and intense absorption band characteristic of blue $CoAl_2O_4$ spinels, which appears between 500 and 650 nm. In this last range the two characteristic transitions of Co^{2+} ion are produced according to Alarcón et al. [37]. The absence of Cr^{3+} ion in $\Psi = 1$ increases the reflectance of the spectrophotometric curve between 350 and 550 nm. There are no changes to remark when $\Psi > 600$ nm, because this emission is typical for Co^{2+} ion. The fuel effect is not quite clear, but Fig. 8 seemed to point out that pigments synthesized with glycine generates glazes with a reflectance curve over the rest of the fuels, indicating that colours have a similar shade but with higher luminosity.

The evolution of glazes' CIELab chromatic coordinates with pigment composition is similar for the three fuels (Fig. 9). L^* coordinate show a minimum approximately when Ψ is around 0.8. Its evolution is progressive for $\Psi < 0.8$, which means that pigments darken progressively when Al^{3+} substitutes Cr^{3+} ion in the structure. However, the luminosity of the glaze increases in respect to the minimum when pigments are free of Cr^{3+} ($\Psi = 1$). a^* coordinate undergoes a sharply variation, evolving from intense green shades when $\Psi = 0$, to red shades as the system increases in Al^{3+}, but this trend intensifies for $\Psi > 0.8$. b^* coordinate for pigments with low content in aluminium corresponds to a bluish shade which slightly losses intensity with Ψ, except for $\Psi > 0.8$, for which the blue component increases significantly.

Some subtle changes in colour development are observed when pigments are synthesized with glycine instead of urea or HMT. The L^* values are higher and b^* values are lower in all the range of compositions, indicating that obtained
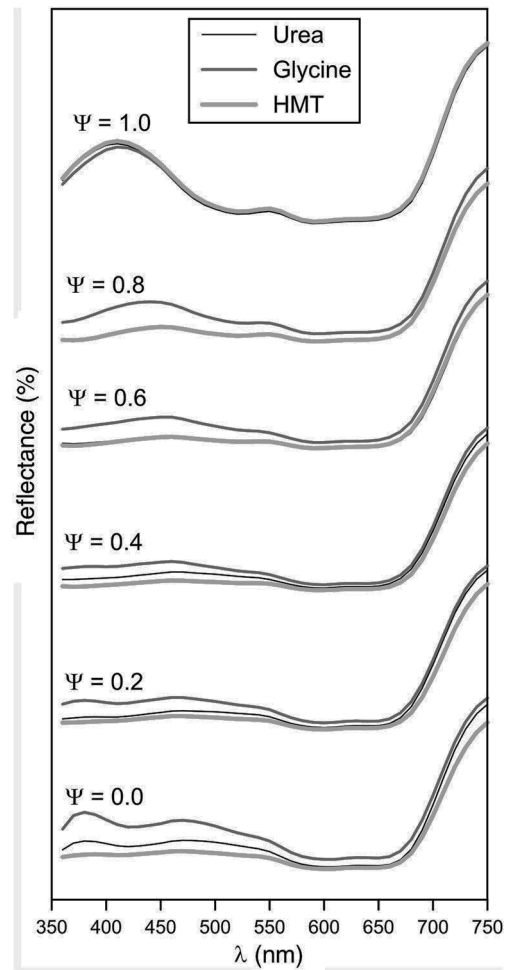

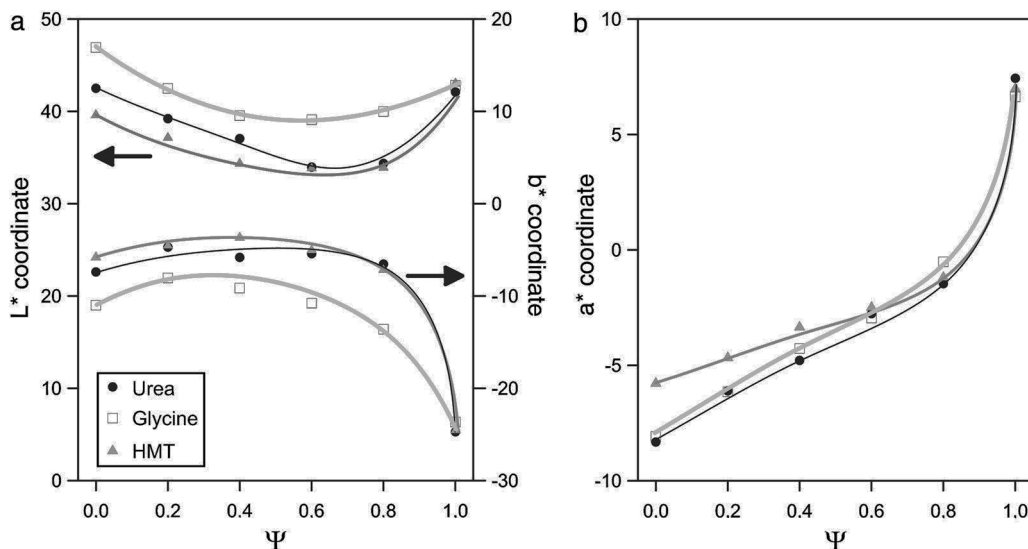Fig. 8 – Reflectance curves of the glazes that contain the synthesized pigments.

Fig. 9 – Evolution of chromatic coordinates of glaze versus the pigment composition: (a) L^* and b^* coordinates and (b) a^* coordinate.

pigments have a little different colouring power. By contrast, the colouring power of the pigments obtained with HMT or urea was very similar. This fact can be interpreted considering that glycine generates the spongiest pigments, which leave the surface grains more exposed to be attacked by the glaze, affecting directly to the intensity of the colour (lighter by the pigment's partial dissolution and bluer by the presence of Co^{2+} dissolved in the glaze). The more compact microstructure of the pigments obtained with urea and HMT offer a better protection against dissolution. In consequence, their colour is darker but with a higher b^* coordinate.

Spinels synthesized in this study show a high and relatively stable colouring power in spite of the differences in microstructure or crystallinity provoked by the fuel used in SCS process. This characteristic is very interesting from an industrial point of view because it opens the door to generate directly pigments suitable for inkjet inks, or at least with lower milling needs than the pigments synthesized by the traditional ceramic process.

Conclusions

SCS technique allows synthesising mixed solid solution pigments between two pure spinels, following the composition $CoCr_{2-2\psi}Al_{2\psi}O_4$ ($0 \leq \Psi \leq 1$ in steps of 0.2). The nature and course of the decomposition products of the fuel and oxidizer seems to control the combustion behaviour.

Highly foamy pigments have been developed, being glycine the one that leads to the most voluminous and fluffy structures. The products showed the spinel-type Fd-3m structure, although in some specific cases some non-integrated aluminium generates oxides, which are highly reactive with water. Accused composition and fuel effects have been observed in crystallinity and crystallite size, whereas lattice parameter was only related with composition. The Cr^{3+}-richest compositions with glycine generated the best crystallized pigments with the highest crystallite size (up to approximately 100 nm). Regarding microstructural aspects, composition and fuel influenced the size and morphology of grains. However, particle size does not show significant variations neither because of composition nor fuel used, being the milling process the unique that controls the final particle size.

Finally, as far as colour development is concerned, all samples develop intense tones, with a high colouring power when added to a ceramic glaze, meaning good stability to be used as ceramic pigments. Cr-rich pigments allow obtaining higher green component while Al-rich spinels develop tones towards the blue component. Fuel effect has been only noticeable when brighter tones are wanted to be developed. Glycine generates the spongiest pigments with grains more exposed to be attacked by the glaze, affecting directly to the intensity of the colour, obtaining brighter colour hues.

SCS pigments are demonstrated to show high stability against temperature, fuel and glaze attack, which made it a suitable alternative to traditional process. Glycine fuel has revealed as the most suitable alternative to obtain pigments so as to be used in inkjet technology.

REFERENCES

[1] P. Escribano, J.B. Carda, E. Cordoncillo, Esmaltes y pigmentos cerámicos, Faenza Editrice, Castellón, 2001.

[2] S. Sanjabi, A. Obeydavi, Synthesis and characterization of nanocrystalline $MgAl_2O_4$ spinel via modified sol–gel method, J. Alloys Compd. 645 (2015) 535–540, http://dx.doi.org/10.1016/j.jallcom.2015.05.107

[3] P. Escribano, M. Marchala, M.L. Sanjuán, P. Alonso-Gutiérrez, B. Julián, E. Cordoncillo, Low-temperature synthesis of $SrAl_2O_4$ by a modified sol–gel route: XRD and Raman characterization, J. Solid State Chem. 178 (2005) 1978–1987, http://dx.doi.org/10.1016/j.jssc.2005.04.001

[4] I.V. Pishch, E.V. Radion, Use of the precipitation method in the synthesis of ceramic pigments, Glass Ceram. 62 (2005) 9–191, http://dx.doi.org/10.1007/s10717-005-0069-2

[5] I.V. Pishch, E.V. Radion, A pigment based on coprecipitated iron(III) and nickel(III) hydroxides, Glass Ceram. 53 (1996) 178–179, http://dx.doi.org/10.1007/BF01166033

[6] R.A. Candeia, M.A.F. Souza, M.I.B. Bernardi, S.C. Maestrelli, I.M.G. Santos, A. Souza, et al., $MgFe_2O_4$ pigment obtained at low temperature, Mater. Res. Bull. 41 (2006) 183–190, http://dx.doi.org/10.1016/j.materresbull.2005.07.019

[7] L.K.C. de Souza, J.R. Zamian, G.N. da Rocha, L.E.B. Soledade, I.M.G. dos Santos, et al., Blue pigments based on $Co_xZn_{1-x}Al_2O_4$ spinels synthesized by the polymeric precursor method, Dyes Pigments 81 (2009) 187–192, http://dx.doi.org/10.1016/j.dyepig.2008.09.017

[8] L. Gama, M.A. Ribeiro, B.S. Barros, R.H.A. Kiminami, I.T. Weber, A.C.F.M. Costa, Synthesis and characterization of the $NiAl_2O_4$, $CoAl_2O_4$ and $ZnAl_2O_4$ spinels by the polymeric precursors method, J. Alloys Compd. 483 (2009) 453–455, http://dx.doi.org/10.1016/j.jallcom.2008.08.111

[9] K.C. Patil, M.S. Hedge, T. Rattan, S.T. Aruna, Chemistry of Nanocrystalline Oxide Materials: Combustion Synthesis, Properties and Applications, World Scientific Publishing, Singapore, 2008.

[10] K. Suresh, K.C. Patil, A combustion process for the instant synthesis of α-Fe_2O_3, J. Mater. Sci. Lett. 12 (1992) 572–574, http://dx.doi.org/10.1007/BF00278328

[11] J.J. Kingsley, K.C. Patil, A novel combustion process for the synthesis of fine particle α-alumina and related oxide materials, Mater. Lett. 6 (1988) 427–432, http://dx.doi.org/10.1016/0167-577X(88)90045-6

[12] S.T. Aruna, K.C. Patil, Synthesis and properties of nanosized titania, J. Mater. Synth. Process. 4 (1996) 175–176.

[13] M.S. Nagaveni, G. Hedge, Structure and photocatalytic activity of $Ti_{1-x}M_xO_{2-\delta}$ (M = W, V, Ce, Zr, Fe and Cu) synthesized by solution combustion method, J. Phys. Chem. B 108 (2004) 20204–20212, http://dx.doi.org/10.1021/jp047917v

[14] M.A. Rodríguez, C.L. Aguilar, M.A. Aghayan, Solution combustion synthesis and sintering behaviour of $CaAl_2O_4$, Ceram. Int. 38 (2012) 395–399, http://dx.doi.org/10.1016/j.ceramint.2011.07.020

[15] B.M. Nagabhushana, R.P.S. Chankrandhar, K.P. Ramesh, C. Shivakumara, G.T. Chandrappa, Combustion synthesis, characterization and metal-insulator transition studies of nanocrystalline $La_{1-x}Ca_xMnO_3$ ($0 \leq X \leq 0.5$), Mater. Chem.

Phys. 102 (2007) 47–52, http://dx.doi.org/10.1016/j.matchemphys.2006.11.002

[16] Color Pigments Manufacturers Association (CPMA), Classification and Chemical Descriptions of the Complex Inorganic Color Pigments, 4th ed., CPMA, Alexandria, VA, 2013.

[17] K. Suresh, N.R.S. Kumar, K.C. Patil, A novel combustion synthesis of spinel ferrites, orthoferrites and garnets, Adv. Mater. 3 (1991) 148–150, http://dx.doi.org/10.1002/adma.19910030306

[18] S.S. Manoharan, K.C. Patil, Combustion synthesis of metal chromite powders, J. Am. Ceram. Soc. 75 (1992) 1012–1015, http://dx.doi.org/10.1111/j.1151-2916.1992.tb04177.x

[19] A.C.F.M. Costa, A.M.D. Leite, H.S. Ferreira, R.H.G.A. Kiminami, S. Cava, L. Gama, Brown pigment of the nanopowder spinel ferrite prepared by combustion reaction, J. Eur. Ceram. Soc. 28 (2008) 2033–2037, http://dx.doi.org/10.1016/j.jeurceramsoc.2007.12.039

[20] R. Ianoş, R. Lazău, P. Barvinschi, Synthesis of $Mg_{1-x}Co_xAl_2O_4$ blue pigments via combustion route, Adv. Powder Technol. 22 (2011) 396–400, http://dx.doi.org/10.1016/j.apt.2010.06.006

[21] T. Mimani, S. Ghosh, Combustion synthesis of cobalt pigments: blue and pink, Curr. Sci. India 78 (2000) 892–896.

[22] S. Mestre, M.D. Palacios, P. Agut, Solution combustion synthesis of $(Co,Fe)Cr_2O_4$ pigments, J. Eur. Ceram. Soc. 32 (9) (2012) 1995–1999, http://dx.doi.org/10.1016/j.jeurceramsoc.2011.11.044

[23] J. Gilabert, M.D. Palacios, V. Sanz, S. Mestre, Characteristics reproducibility of $(Fe,Co)(Cr,Al)_2O_4$ pigments obtained by solution combustion synthesis, Ceram. Int. 42 (2016) 12880–12887, http://dx.doi.org/10.1016/j.ceramint.2016.05.054

[24] M.C. Gardey Merino, A.L. Estrella, M.E. Rodriguez, L. Acuña, M.S. Lassa, G.E. Lascalea, P. Vázquez, Combustion syntheses of $CoAl_2O_4$ powders using different fuels, Procedia Mater. Sci. 8 (2015) 519–525, http://dx.doi.org/10.1016/j.mspro.2015.04.104

[25] K. Christine Stella, A. Samson Nesaraj, Effect of fuels on the combustion synthesis of $NiAl_2O_4$ spinel particles, Iran. J. Mater. Sci. Eng. 7 (2) (2010) 36–44.

[26] M. Llusar, A. Forés, J.A. Badenes, J. Calbo, M.A. Tena, G. Monrós, Colour analysis of some cobalt-based blue pigments, J. Eur. Ceram. Soc. 21 (2001) 1121–1130, http://dx.doi.org/10.1016/S0955-2219(00)00295-8

[27] S.A. Eliziário, M.A. Jeferson, S.J.G. Limac, C.A. Paskocimas, L.E.B. Soledade, P. Hammer, E. Longoa, A.G. Souza, I.M.G. Santos, Black and green pigments based on chromium–cobalt spinels, Mater. Chem. Phys. 129 (2011) 619–624, http://dx.doi.org/10.1016/j.matchemphys.2011.05.001

[28] K.E. Sickafus, J.M. Wills, Structure of spinel, J. Am. Ceram. Soc. 82 (1999) 3279–3292, http://dx.doi.org/10.1111/j.1151-2916.1999.tb02241.x

[29] A. Samson Nesaraj, Studies on materials and components for the intermediate temperature solid oxide fuel cells (ITSOFC) (Ph.D. thesis), Alagappa University, India, 2002.

[30] International Center for Diffraction Data (ICDD) PDF-4+ file, ICDD 04-014-1636.

[31] International Center for Diffraction Data (ICDD) PDF-4+ file, ICDD 04-008-3316.

[32] D.R. Lide (Ed.), CRC Handbook of Chemistry and Physics, 74th ed., CRC Press, Boca Raton, 1993.

[33] J. Shou-Yong, L.Z. Jin, L. Yong, Investigation on lattice constants of Mg-Al spinels, J. Mater. Sci. Lett. 19 (2000) 225–227, http://dx.doi.org/10.1023/A:1006710808718

[34] I.C. Nlebedim, J.E. Snyder, A.J. Moses, D.C. Jiles, Effect of deviation from stoichiometric composition on structural and magnetic properties of cobalt ferrite, $Co_xFe_{3x}O_4$ ($x = 0.2$ to 1.0), J. Appl. Phys. 111 (2012) 07D704, http://dx.doi.org/10.1063/1.3670982

[35] D.N. Todor, Thermal Analysis of Minerals, Abacus Press, Tunbridge Wells, 1976.

[36] M.P. Gómez-Tena, J. Gilabert, J. Toledo, E. Zumaquero, C. Machí, Relationship between the specific surface area parameters determined using different analytical techniques, in: Qualicer 2014: XIII World Congress on Ceramic Tiles, Cámara Oficial de Comercio, Industria y Navegación, Castellón, 2014.

[37] J. Alarcón, P. Escribano, R.Mª Marín, Co(II) based ceramic pigments, Br. Ceram. Trans. J. 84 (1985) 170–172.